

SYNTHESIS AND CHARACTERIZATION OF CELLULOSE-SILICA COMPOSITE FIBER IN ETHANOL/WATER MIXED SOLVENTS

Ning Jia,^a Shu-Ming Li,^a Ming-Guo Ma,^{a*} Jie-Fang Zhu,^b and Run-Cang Sun^{a,*}

Cellulose-silica composite fiber samples have been successfully synthesized using cellulose solution, tetraethoxysilane, and $\text{NH}_3 \cdot \text{H}_2\text{O}$ in ethanol/water mixed solvents at room temperature for 24 h. The cellulose solution was previously prepared by the dissolution of microcrystalline cellulose in a solvent mixture of N,N-dimethylacetamide (DMAc)/lithium chloride (LiCl). The effect of the tetraethoxysilane concentration on the product was investigated. The products were characterized by X-ray powder diffraction (XRD), thermogravimetric analysis (TG), differential scanning calorimetric analysis (DSC), scanning electron microscopy (SEM), Fourier transform infrared spectrometry (FT-IR), energy-dispersive X-ray spectrum (EDS), and cross polarization magic angle spinning (CP/MAS) solid state ^{13}C -NMR. The morphology of the cellulose-silica composite fiber was investigated by SEM, while their composition was established from EDS measurements combined with the results of FT-IR spectral analysis and XRD patterns. The XRD, FT-IR and EDS results indicated that the obtained product was cellulose-silica composite fiber. The SEM micrographs showed that the silica particles were homogeneously dispersed in the cellulose fiber. The CP/MAS solid state ^{13}C -NMR results indicated that the silica concentration had an influence on the crystallinity of the cellulose. This method is simple for preparation of cellulose-based composites.

Keywords: Cellulose; Silica; Composite; Fiber; Microstructure

Contact information: a: Institute of Biomass Chemistry and Technology, College of Materials Science and Technology, Beijing Forestry University, Beijing 100083, P.R. China; b: Department of Materials Chemistry, The Ångström Laboratory, Uppsala University, Uppsala 75121, Sweden. * Corresponding author: mg_ma@bjfu.edu.cn (M.-G. Ma), rcsun3@bjfu.edu.cn (R.-C. Sun).

INTRODUCTION

In the past decade, research on polymer-based composites has become an active field because of their intriguing optical, electrical, magnetic, and mechanical properties (Qiao et al. 1999; Chen et al. 2000; Pyun 2007; Zhu et al. 2007; Magalhaes 2009). These composites are considered to be functional materials with wide potential applications in many fields (Dirix et al. 1999; Sarma et al. 2002; Schurmann et al. 2005). The development of simple and low-cost methods for synthesis of these composites is very important in order to be able to realize their large-scale production and applications.

As an abundant polymer in nature, cellulose has mechanical strength, biocompatibility, biodegradation, low toxicity, and high chemical durability due to the strong intra- and inter-molecular hydrogen bonding (Miyamoto et al. 1989; Sveinsson et al. 2005). Recently the synthesis of cellulose-based composites has received considerable attention, and many efforts have been focused on it. Until now, the fabrication of the

cellulose-based composites including cellulose/TiO₂ (Daoud et al. 2005; Marques et al. 2006; Zhou et al. 2006), cellulose/Fe₂O₃ (Liu et al. 2006, 2008), cellulose/hydroxyapatite (Tsiptsias et al. 2008), cellulose/polymerized ionic liquid (Murakami et al. 2007), and cellulose/carbon-nanotube (Zhang et al. 2007) have been reported.

Silica has been extensively studied for its potential applications in various fields such as catalytic supports, sensors, optical hosts, and sorption media (Kresge et al. 1992; Bunker et al. 1994; Corma 1997). However, there have been only few reports on the fabrication of cellulose-silica composites (Dun et al. 2003; Hribernik et al. 2007; Pinto et al. 2008). The preparation and mechanical properties of bacterial cellulose composites loaded with silica nanoparticles were reported by Yano et al. (2008).

Herein, we report a facile route to the synthesis of cellulose-silica composite fiber using cellulose solution, tetraethoxysilane, and NH₃•H₂O in ethanol/water mixed solvents at room temperature for 24 h. The cellulose solution was previously prepared by the dissolution of microcrystalline cellulose in a solvent system of lithium chloride (LiCl)/*N,N*-dimethylacetamide (DMAc). The synthesis of cellulose-silica composites by simultaneous formation of silica particles and the precipitate of cellulose in LiCl/DMAc solution may be favorable for the preparation of a composite of cellulose and silica. Earlier we reported the synthesis of cellulose-calcium silicate nanocomposites in ethanol/water mixed solvents (Li et al. 2010). The ethanol/water mixed solvents favored the fabrication of cellulose-based composites with good dispersion.

EXPERIMENTAL

Materials

All chemicals were of analytical grade and used as received without further purification. All experiments were conducted under air atmosphere. Microcrystalline cellulose (molecular weight of 34,843 to 38,894 Daltons, with a degree of polymerization of 215 to 240) was obtained from Sinopharm Group Chemical Reagent Co., Ltd., Shanghai, China. *N,N*-dimethylacetamide (DMAc), lithium chloride (LiCl), ammonia solution, and tetraethoxysilane were purchased from Beijing Chemical Works.

Methods

A typical synthesis experiment for the cellulose solution was carried out as follows: microcrystalline cellulose (1.416 g) and LiCl (1.510 g) were added into *N,N*-dimethylacetamide (20 mL, DMAc) under vigorous stir at 90 °C for 3 h. The obtained cellulose solution was used for the preparation of cellulose-silica composite fiber.

For the synthesis of cellulose-silica composite fiber, the above obtained cellulose solution (5 mL) was dropped into the ethanol (50 mL)/distilled water (10 mL) mixed solvents, and then 2 mL of ammonia solution (25 wt %) and tetraethoxysilane (1 mL, TEOS, (C₂H₅)₄SiO₄) were rapidly added into the resulting colloidal solution under vigorous stir at room temperature for 24 h. The resulting precipitate was separated from the solution by centrifugation, washed by water and ethanol several times, and dried at 60 °C for further characterization. The cellulose-silica composite fiber was obtained.

Characterization

X-ray diffractometer (XRD) patterns were recorded on an X'Pert PRO MPD diffractometer operating at 40 kV with Cu K α ($\lambda = 1.5405 \text{ \AA}$) radiation. Thermal behavior of the cellulose-silica composite was performed using thermogravimetric analysis (TG) and differential scanning calorimetric analysis (DSC) with a STA-409PC/4/H Luxx simultaneous TG-DTA/DSC apparatus (Netzsch, Germany) at a heating rate of $10 \text{ }^\circ\text{C min}^{-1}$ in flowing air. An FT-IR spectrophotometer (Nicolet 510) was used to identify the ingredients of the composites, using the KBr disk method. The morphology of cellulose-silica composites was examined using a Hitachi 3400 N scanning electron microscopy (SEM). The energy-dispersive X-ray spectra (EDS) attached to the scanning electron microscopy was used to analyze the composition of sample. Solid-state ^{13}C cross-polarization magic angle spinning (CP/MAS) NMR spectra were obtained on a Bruker AVIII 400 MHz spectrometer. The relative ratio of crystalline fraction to amorphous fraction of cellulose was calculated by using peaks area from NMR spectrum of C-4.

RESULTS AND DISCUSSION

The XRD pattern of the regenerated cellulose is shown in Fig. 1a, with the diffraction peaks at $2\theta = \sim 20.46^\circ$ and 22.58° , assigned to the (110) and (200) planes of the cellulose type I. Fig. 1b shows the XRD pattern of the typical cellulose-silica composite fiber, which exhibited similar diffraction peaks, compared with Fig. 1a.

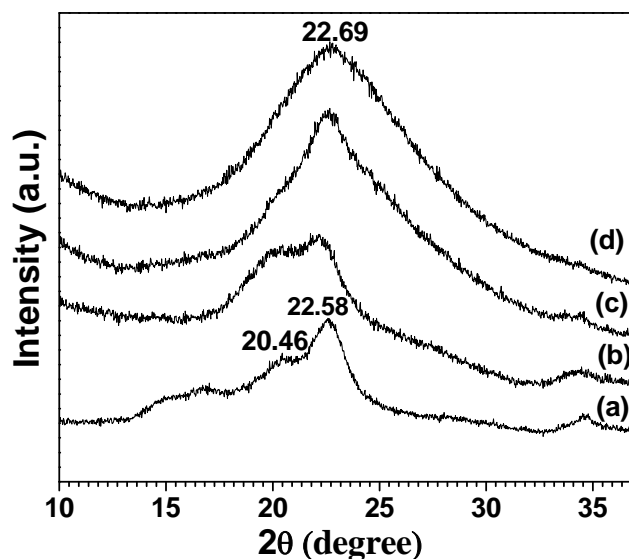


Fig. 1. XRD patterns of (a) the regenerated cellulose, (b-d) the typical cellulose-silica composite fiber synthesized using different TEOS concentrations at room temperature for 24 h: (b) 1 mL; (c) 5 mL; (d) 10 mL

When the TEOS concentrations were increased to 5 mL and 10 mL, the amorphous characteristic of silica centered at $2\theta = \sim 22.69^\circ$ was observed, as shown in Fig. 1c and d, respectively. The diffraction peaks as the typical diffraction pattern of cellulose type II were not clearly observed in Fig. 1c and d because of the overlapping with the strong band at around 22.69° .

The thermal behavior of the cellulose-silica composite fiber was further investigated with thermogravimetric analysis (TG) and differential scanning calorimetric analysis (DSC). The TG curve shown in Fig. 2a indicates that the total weight loss amounted to 88 %. This includes three weight loss stages: the weight loss below 220°C is due to the desorption of water, whereas the significant weight losses from 220 to 270°C and 270 to 680°C were attributed to the thermal degradation and complete decomposition of cellulose in the composites, respectively. Similar observations in which two weight loss stages of cellulose observed in cellulose-based composites were earlier reported for cellulose-hydroxyapatite composites (Ma et al. 2010), cellulose-Ag composites (Li et al. 2010), and cellulose-carbonated hydroxyapatite composites (Jia et al. 2010). This phenomenon was possibly due to a strong interaction between inorganic particles and the cellulose matrix. A small endothermic peak was observed at around 94°C in the DSC curve (Fig. 2b). Moreover, a broad exothermic peak was displayed in the region 350 to 700°C , which fits well with the biggest weight loss in the TG curve. The degradation temperature in the cellulose-silica composite fiber was different from the regenerated cellulose, which took place in the region 190 to 310°C (Li et al. 2009), indicating that the formation of the composites had an effect on the thermal stability of regenerated cellulose.

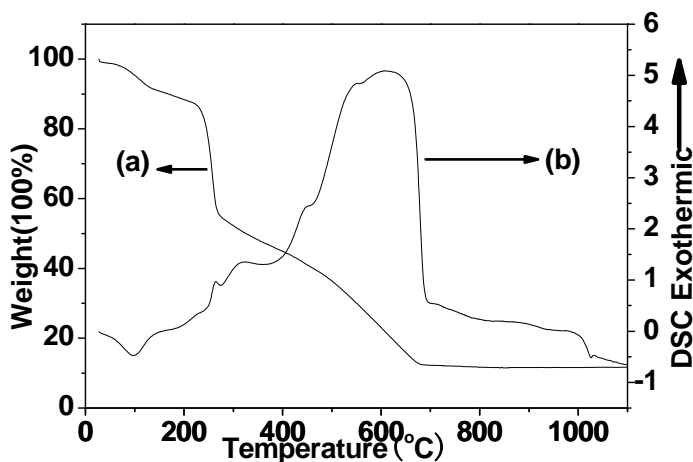


Fig. 2. TG(a) and DSC(b) curves of the typical cellulose-silica composite fiber

Figure 3 shows the Fourier transform infrared (FT-IR, Nicolet 510) spectra of the cellulose-silica composite fiber, the regenerated cellulose, and pure microcrystalline cellulose. The IR spectrum of the pure microcrystalline cellulose (Fig. 3a) shows a strong broad band at ca. 3390 cm^{-1} , and a band at 1636 cm^{-1} corresponding to the stretching and bending modes of the surface hydroxyls; the peak at 2905 cm^{-1} belongs to the asymmetrically stretching vibration of C-H in a pyranoid ring, and the broad absorption

peak ca. 1059 cm^{-1} is attributed to the C-O of cellulose. The regenerated cellulose exhibited similar peaks compared to Fig. 3a. However, the peaks intensity decreased, as shown in Fig. 3b. The IR spectrum of the composite fiber showed adsorption at ca. 465 cm^{-1} (Fig. 3c), which is a typical characteristic peak for silica materials and belongs to the bending mode of the Si-O bond. The band at ca. 960 cm^{-1} is attributed to the symmetric stretching vibration of the Si-OH headgroup. The peaks around 800 and 1097 cm^{-1} are related to the symmetric vibration and asymmetric vibration of Si-O-Si in SiO_4 tetrahedra (Boissière et al. 2000). The characteristic stretching mode of the C-O in cellulose is not clearly observed because of the overlapping with the strong band of the asymmetric vibration of O-Si-O bonds (1097 cm^{-1}). The band at ca. 1636 cm^{-1} is due to the bending mode of water, and the band at ca. 3430 cm^{-1} can be assigned to surface hydroxylation OH stretching mode, implying the presence of adsorbed water. Moreover, the peak at ca. 3390 cm^{-1} of cellulose moved to a higher wavenumber ($\sim 3430\text{ cm}^{-1}$) and became broader in the composites. These IR results indicated the existence of the silica in composites fiber and a strong interaction between the OH groups of cellulose and silica particles. As is well known, cellulose has many surface hydroxyls, which contribute to the polymer's stiffness and close chain packing via numerous intermolecular and intramolecular hydrogen bonds. Colloidal silica particles are bound to cellulose by surface hydroxyls. A similar phenomenon was reported for cellulose- Fe_2O_3 composites (Liu et al. 2008b).

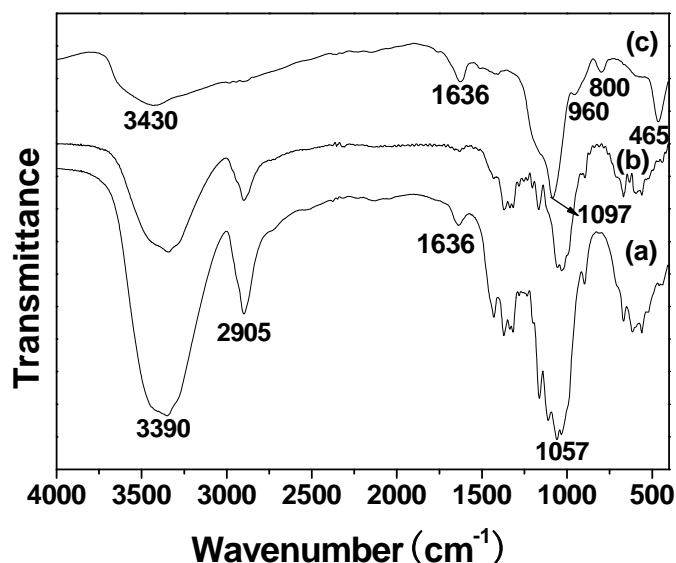


Fig. 3. FT-IR spectra of (a) the microcrystalline cellulose, (b) the regenerated cellulose and (c) the cellulose-silica composite fiber

The morphologies of the cellulose-silica composite fiber were investigated with scanning electron microscopy (SEM, Hitachi 3400N). Figure 4a,b shows SEM micrographs of the cellulose-silica composites with fiber-like morphology. A magnified micrograph of the composite fiber is shown in Fig. 4c. One can see that the silica particles were relatively homogeneously dispersed in the cellulose matrix, which had a

rolling morphology. The detailed structure of the composite fiber is shown in Fig. 4d. The fiber formation also occurred for regenerated cellulose without TEOS addition. The cellulose solution in a solvent mixture of DMAc/LiCl had high viscosity. When the cellulose solution was added into the ethanol/distilled water mixed solvents, the regenerated cellulose immediately precipitated, forming fiber. When the TEOS was added, the silica particles covered the surface of the regenerated cellulose fiber. The energy-dispersive X-ray spectrum (Fig. 5) shows that the sample consisted of C, O, and Si, and the determined composition was consistent with that of cellulose-silica composite fiber, which further confirmed the formation of cellulose-silica composite fiber. The peak intensity of C was weak due to the silica covering the surface of the regenerated cellulose.

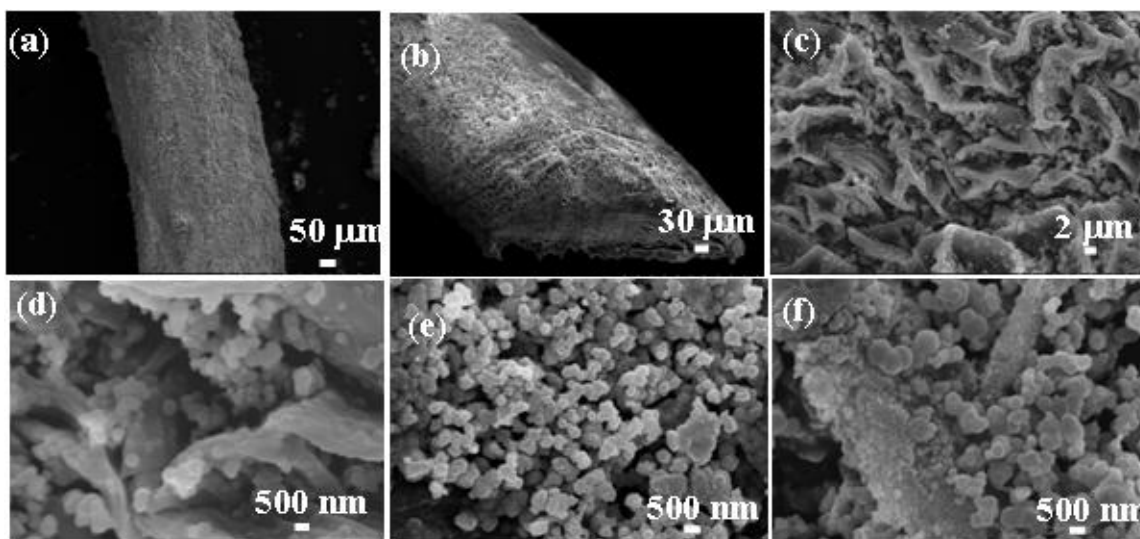


Fig. 4. SEM micrographs of the cellulose-silica composite fiber prepared using different TEOS concentrations at room temperature for 24 h: (a-d) 1 mL; (e) 5 mL; (f) 10 mL

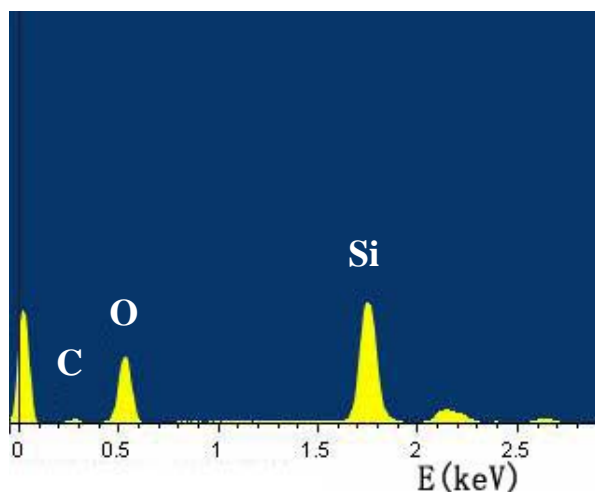


Fig. 5. EDS spectrum of the cellulose-silica composite fiber

The TEOS concentration had a significant effect on the size and morphology of silica particles in the composite fiber. When the TEOS concentration was 5 mL, the size of the silica in the composite fiber was obviously increased, and the silica particles were mostly more visible (Fig. 4e), compared with Fig. 4a-d. When the TEOS concentration was increased to 10 mL, the silica particle size was increased, and spheres were observed (Fig. 4f).

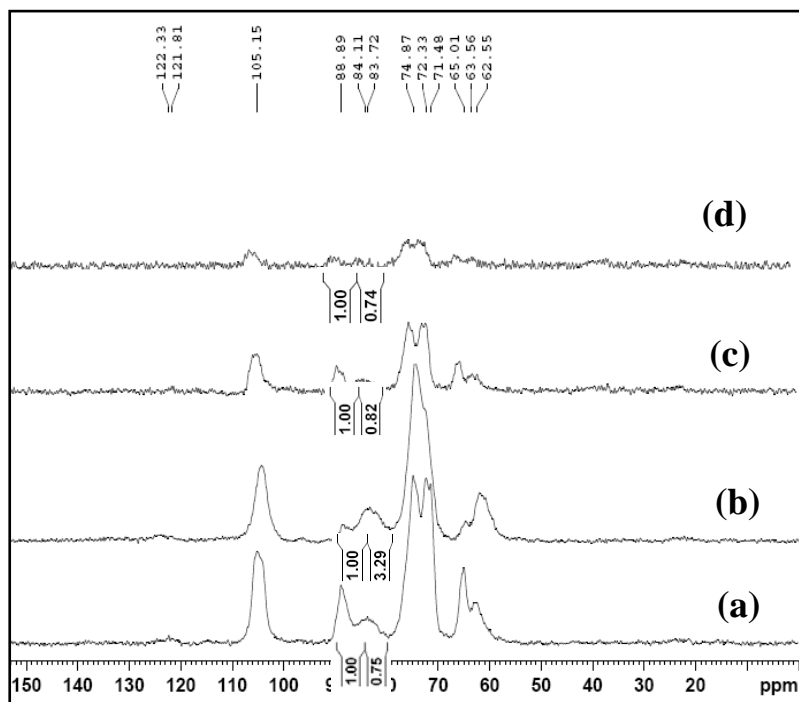


Fig. 6. CP/MAS ^{13}C -NMR spectra of the cellulose-silica composite fiber prepared using different TEOS concentrations at room temperature for 24 h: (a) the regenerated cellulose; (b) 1 mL; (c) 5 mL; and (d) 10 mL

Figure 6b shows the cross polarization magic angle spinning (CP/MAS) ^{13}C solid state NMR spectrum of a typical sample prepared using 1 mL TEOS at room temperature for 24 h. The signals at (62.8+65.5), 75.3, (97.1+97.5), and 104.5 ppm are attributed to C-6, C2-C3-C5, C-4, and C-1, respectively (Zawadzki and Wisniewski 2002). In addition, the small peaks at about 62.8 and 97.1 ppm are the contribution of the disordered regions for C6 and C4 carbons; the peaks at about 65.5 and 97.5 ppm stand for the ordered regions for C6 and C4 carbons, respectively (Liitiä et al. 2000). The crystalline fraction reached a value of 23.31%, the amorphous fraction was 76.69%, and the ratio calculated from NMR spectrum of C-4 was 1:3.29, as shown in Fig. 6a. For comparison, the CP/MAS ^{13}C solid state NMR spectrum of the regenerated cellulose is also shown in Fig. 6a. One can see that the ratio calculated from the NMR spectrum of C-4 was 1:0.75, indicating that the crystalline fraction decreased with the addition of silica particles. Moreover, the CP/MAS ^{13}C solid state NMR spectrum of the cellulose-silica composite fiber synthesized using 5 mL and 10 mL TEOS at room temperature for 24 h is also shown in Fig. 6 c and d, respectively. One can see that the peaks at around 75.3 ppm for C2-C3-C5 were split, and the intensity peaks decreased compared with Fig. 6b. The

crystallinity value was increased from 23.31% to 54.94% and 57.47%, respectively. The intensity of peaks decreased with increasing silica concentration. This result indicates that the silica concentration has an influence on the crystallinity of cellulose, and the incorporated silica particles led to a decrease of the crystallinity of the cellulose in composite fiber. Of course, the intrinsic mechanism needs to be further explored.

CONCLUSIONS

1. A facile method has been successfully used for the preparation of cellulose-silica composite fiber in ethanol/water mixed solvents at room temperature for 24 h.
2. From the SEM results it can be concluded that the silica particles were homogeneously dispersed in the cellulose matrix.
3. The EDS spectrum further confirmed the formation of cellulose-silica composite fiber.
4. CP/MAS ^{13}C solid state NMR spectra indicated that the incorporated silica particles led to a decrease of the crystallinity of the cellulose in composite fiber.
5. The TEOS concentration had a significant effect on the size and morphology of silica particles in the composite fiber.

ACKNOWLEDGMENTS

Financial support from the National Natural Science Foundation of China (31070511), Research Fund for the Doctoral Program of Higher Education of China (20100014120010), China Postdoctoral Science Special Foundation (201003059), and Major State Basic Research Development Program of China (973 Program) (No.2010CB732204) is gratefully acknowledged.

REFERENCES CITED

- Boissière, C., Larbot, A., Lee, A., Kooyman, P. J., and Prouzet, E. (2000). "A new synthesis of mesoporous MSU-X silica controlled by a two-step pathway," *Chem.Mater.* 12, 2902-2913.
- Bunker, B. C., Rieke, P. C., Tarasevich, B. J., Campell, A. A., Fryxell, G. E., and Graff, G. L. (1994). "Ceramic thin-film formation on functionalized interfaces through biomimetic processing," *Science* 264, 48-55.
- Chen, M., Xie, Y., Qiao, Z. P., Zhu, Y. J., and Qian, Y. T. (2000). "Synthesis of short CdS nanofiber/poly(styrene-alt-maleic anhydride) composites using γ -irradiation," *J. Mater.Chem.* 10, 329-332.
- Corma, A. (1997). "From microporous to mesoporous: Molecular sieve materials and their use in catalysis," *Chem. Rev.* 97, 2373-2420.

- Daoud, W. A., Xin, J. H., and Zhang, Y. H. (2005). "Surface functionalization of cellulose fibers with titanium dioxide nanoparticles and their combined bactericidal activities," *Surf. Sci.* 599, 69-75.
- Dirix, Y., Bastiaansen, C., Caseri, W., and Smith, P. (1999). "Oriented pearl-necklace arrays of metallic nanoparticles in polymers: a new route toward polarization-dependent color filters," *Adv. Mater.* 11, 223-227.
- Dun, H. J., Song, X. Q., Liu, Y. Q., and Chen, L. R. (2003). "Preparation of derivatized cellulose coated ZrO_2/SiO_2 and direct chiral resolution of a-biphenyl dicarboxylate compounds by HPLC," *Acta Chimica Sinica* 61, 1326-1330.
- Hribernik, S., Smole, M. S., Kleinschek, K. S., Bele, M., Jamnik, J., and Gaberscek, M. (2007). "Flame retardant activity of SiO_2 -coated regenerated cellulose fibres," *Polym. Degrad. Stabil.* 92, 1957-1965.
- Jia, N., Li, S. M., Ma, M. G., Sun, R. C., and Zhu, J. F. (2010). "Hydrothermal synthesis and characterization of cellulose-carbonated hydroxyapatite nanocomposites in NaOH-urea aqueous solution," *Sci. Adv. Mat.* 2, 210-214.
- Kresge, C. T., Leonowicz, M. E., Roth, W. J., Vartuli, J. C., and Beck, J. S. (1992). "Ordered mesoporous molecular sieves synthesized by a liquid-crystal template mechanism," *Nature* 359, 710-712.
- Li, S. M., Jia, N., Zhu, J. F., Ma, M. G., and Sun, R. C. (2010). "Synthesis of cellulose-calcium silicate nanocomposites in ethanol/water mixed solvents and their characterization," *Carbohydr. Polym.*, 80, 270-275.
- Li, S. M., Jia, N., Zhu, J. F., Ma, M. G., Xu, F., Wang, B., and Sun, R. C. (2011). "Rapid microwave-assisted preparation and characterization of cellulose-silver nanocomposites," *Carbohydr. Polym.* 83, 422-429.
- Liu, S. L., Zhang, L. N., Zhou, J. P., Xiang, J. F., Sun, J. T., and Guan, J. G. (2008a). "Fiberlike Fe_2O_3 macroporous nanomaterials fabricated by calcinating regenerate cellulose composite fibers," *Chem. Mater.* 20, 3623-3628.
- Liu, S. L., Zhang, L. N., Zhou, J. P., and Wu, R. X. (2008b). "Structure and properties of cellulose/ Fe_2O_3 nanocomposite fibers spun via an effective pathway," *J. Phys. Chem. C* 112, 4538-4544.
- Liitiä, T., Maunu, S. L., and Hortling, B. (2000). "Solid state NMR studies on cellulose crystallinity in fines and bulk fibres separated from refined kraft pulp," *Holzforschung*, 54, 618-624.
- Liu, S. L., Zhou, J. P., Zhang, L. N., Guan, J. G., and Wang, J. B. (2006). "Synthesis and alignment of iron oxide nanoparticles in a regenerated cellulose film," *Macromol. Rapid Commun.* 27, 2084-2089.
- Ma, M. G., Zhu, J. F., Jia, N., Li, S. M., Sun, R. C., Cao, S. W., and Chen, F. (2010). "Rapid microwave-assisted synthesis and characterization of cellulose-hydroxyapatite nanocomposites in *N,N*-dimethyl-acetamide solvent," *Carbohydr. Res.* 345, 1046-1050.
- Magalhaes, W. L. E., Cao, X. D., and Lucia, L. A. (2009). "Cellulose nanocrystals/cellulose core-in-shell nanocomposite assemblies," *Langmuir* 25, 13250-13257.

- Marques, P. A. A., Trindade, T., and Neto, C. P. (2006). "Titanium dioxide/cellulose nanocomposites prepared by a controlled hydrolysis method," *Comp. Sci. Techn.* 66, 1038-1044.
- Miyamoto, T., Takahashi, S., Ito, H., and Inagaki, H. (1989). "Tissue biocompatibility of cellulose and its derivatives," *J. Biomed. Mater. Res.*, 23, 125-133.
- Murakami, M., Kaneko, Y., and Kadokawa, J. (2007). "Preparation of cellulose-polymerized ionic liquid composite by in-situ polymerization of polymerizable ionic liquid in cellulose-dissolving solution," *Carbohydr. Polym.* 69, 378-381.
- Pinto, R. J. B., Marques, P. A. A. P., Barros-Timmons, A. M., Trindade, T., and Neto, C. P. (2008). "Novel SiO₂/cellulose nanocomposites obtained by *in situ* synthesis and *via* polyelectrolytes assembly," *Comp. Sci. Technol.*, 68, 1088-1093.
- Pyun, J. (2007). "Nanocomposite materials from functional polymers and magnetic colloids," *Polym. Rev.* 4, 231-263.
- Qiao, Z. P., Xie, Y., Zhu, Y. J., and Qian, Y. T. (1999). "Synthesis of PbS/polyacrylonitrile nanocomposites at room temperature by γ -irradiation," *J. Mater. Chem.* 9, 1001-1002.
- Sarma, T. K., Chowdhury, D., Paul, A., and Chattopadhyay, A. (2002). "Synthesis of Au nanoparticle-conductive polyaniline composite using H₂O₂ as oxidising as well as reducing agent," *Chem. Commun.* 1048-1049.
- Schurmann, U., Hartung, W. A., Takele, H., Zaporozhchenko, V., and Faupel, F. (2005). "Controlled syntheses of Ag-polytetrafluoroethylene nanocomposite thin films by co-sputtering from two magnetron sources," *Nanotechnology* 16, 1078-1082.
- Sveinsson, A., Nicklasson, E., Harrah, T., Panilaitis, B., Kaplan, D. L., and Brittberg, M., (2005). "Bacterial cellulose as a potential scaffold for tissue engineering of cartilage," *Biomaterials* 26, 419-431.
- Tsiptsias, C., and Panayiotou, C. (2008). "Preparation of cellulose-nanohydroxyapatite composite scaffolds from ionic liquid solutions," *Carbohydr. Polym.* 74, 99-105.
- Yano, S., Maeda, H., Nakajima, M., Hagiwara, T., and Sawaguchi, T. (2008). "Preparation and mechanical properties of bacterial cellulose nanocomposites loaded with silica nanoparticles," *Cellulose* 15, 111-120.
- Zawadzki, J., and Wisniewski, M. (2002). "C-13 NMR study of cellulose thermal treatment," *J. Analytical and Appl. Pyrolysis*, 62, 111-121.
- Zhang, H., Wang, Z. G., Zhang, Z. N., Wu, J., Zhang, J., and He, J. S. (2007). "Regenerated cellulose/multi-walled carbon nanotube (MWCNT) composite fibers with enhanced mechanical properties prepared with an ionic liquid 1-allyl-3-methylimidazolium chloride (AmimCl)," *Adv. Mater.*, 19, 698-704.
- Zhou, J. P., Liu, S. L., Qi, J. N., and Zhang, L. N. (2006). "Structure and properties of composite films from cellulose and nanocrystalline titanium dioxide particles," *J. Appl. Polym. Sci.* 101, 3600-3608.
- Zhu, J. F., Zhu, Y. J., Ma, M. G., Yang, L. X., and Gao, L. (2007). "Simultaneous and rapid microwave synthesis of polyacrylamide-metal sulfide (Ag₂S, Cu₂S, HgS) nanocomposites," *J. Phys. Chem. C* 111, 3920-3926.

Article submitted: December 13, 2010; Peer review completed: January 24, 2011;
Revised version received and accepted: February 20, 2011; Published: Feb. 22, 2011.